Elemental signatures of *Australopithecus africanus* teeth reveal seasonal dietary stress

renaud Joannes-Boyau[1,17]*, Justin W. Adams[2,3,17], Christine Austin[4,17], Manish Arora[4], Ian Moffat[5,6], Andy I. r. Herries[3,7], Matthew P. tonge[1], Stefano Benazzi[8,9], Alistair r. evans[10,11], Ottmar Kullmer[12,13], Stephen Wroe[14], Anthony Dosseto[15] & Luca Fiorenza[2,16]

Reconstructing the detailed dietary behaviour of extinct hominins is challenging[1]—particularly for a species such as *Australopithecus africanus*, which has a highly variable dental morphology that suggests a broad diet[2,3]. The dietary responses of extinct hominins to seasonal fluctuations in food availability are poorly understood, and nursing behaviours even less so; most of the direct information currently available has been obtained from high-resolution trace-element geochemical analysis of *Homo sapiens* (both modern and fossil), *Homo neanderthalensis*[4] and living apes[5]. Here we apply high-resolution trace-element analysis to two *A. africanus* specimens from Sterkfontein Member 4 (South Africa), dated to 2.6–2.1 million years ago. Elemental signals indicate that *A. africanus* infants predominantly consumed breast milk for the first year after birth. A cyclical elemental pattern observed following the nursing sequence—comparable to the seasonal dietary signal that is seen in contemporary wild primates and other mammals— indicates irregular food availability. These results are supported by isotopic evidence for a geographical range that was dominated by nutritionally depauperate areas. Cyclical accumulation of lithium in *A. africanus* teeth also corroborates the idea that their range was characterized by fluctuating resources, and that they possessed physiological adaptations to this instability. This study provides insights into the dietary cycles and ecological behaviours of *A. africanus* in response to food availability, including the potential cyclical resurgence of milk intake during times of nutritional challenge (as observed in modern wild orangutans[5]). The geochemical findings for these teeth reinforce the unique place of *A. africanus* in the fossil record, and indicate dietary stress in specimens that date to shortly before the extinction of *Australopithecus* in South Africa about two million years ago.

A. africanus is one of the earliest hominins known to inhabit the South African landscape, living from 3.03–2.61 million years ago (Ma) until sometime between 2.3 and 2.1 Ma[6]. Decades of research on the diet[7–9] and mobility[3] of this species has suggested an unusu- ally high degree of dietary variability (which probably included the consumption of fruits, leaves, grasses, sedges and roots) relative to other hominins, which has led to the interpretation that *A. africanus* lived in a complex range of environments that included open grassland and forest[7]. These interpretations are based principally on the broad range of morphology in putative *A. africanus* specimens, which has tentatively been attributed to the potential occurrence of more than one species of *Australopithecus*[10] within Sterkfontein Member 4 (2.61–2.07 Ma) and Makapansgat Limeworks (3.03–2.61 Ma) assemblages[6] (Extended Data Fig. 1) or to substantial changes in the diet of *A. africanus* over time in response to the substantially changing South African ecosystems of the early Pleistocene (about 2.3–2.1 Ma)[11,12]. Although seasonal changes in ecosystems dominated by tropical grassland (frequently referred to as the savannah biome) are associated with only minor variations in temperature, important oscillations in rainfall produce lengthy dry and wet periods[13]. This has a considerable effect on food availability, and leads to long alternating periods of abundance and scarcity of nutritious food. This cyclical rhythm of dry open grassland in winter and wet blooming woodland in summer has prompted mammals to adapt either by undertaking long annual migrations to more-clement regions or by adopting seasonal strategies in food consumption, including the use of fall-back resources (which have poor nutritional values, and are eaten only when preferred foods are scarce or unavailable)[14,15]. This climatic cycle has consequences for the physiological (for example, nursing, reproduction and infant development) and ecological (for example, diet, grouping of individuals and territory size) behaviour of endemic species—particularly for non-migrating individuals[13–15].

Here we have undertaken elemental mapping of dental tissues of *A. africanus* (Extended Data Fig. 1) to study the dietary intake of off- spring during the early stages of development. Teeth are particularly valuable for reconstructing the early-life history of ancient populations as they contain precise temporal and chemical records that are more resistant than bone to post-burial diagenesis (Extended Data Fig. 2). Mineralization of enamel and dentine occurs incrementally, and thus retains a sequential record of the early-life chemical exposure of an individual—both external and internal (for example, metabolites). Well-preserved elemental and isotopic signals have previously been used to reconstruct trophic levels[1], diet[1,2,8] and migration patterns[3] of early hominins, and even the breastfeeding history of late Pleistocene *Homo*[4] and extant apes[5]. Understanding nursing history is extremely valuable for reconstructing the early life of extinct hominins, and in particular for clarifying when the characteristic early weaning and late maturation of modern humans evolved. Previous work has identified barium in teeth as a reliable marker of maternal milk intake[4]. In general, the barium concentration in dental tissues that are formed prenatally is low, owing to restricted maternal transfer via the placenta[16]. Barium concentration increases after birth with absorption from mother's milk, and then slowly decreases over the weaning process to reach its lowest level when the diet of the infant is based solely on solid food. The decrease in barium with weaning—despite the fact that many plantfoods having higher barium concentrations than are present in mater- nal milk—has previously been attributed to differences in the bioavail- ability of barium in milk compared with non-milk foods[4]. Biochemical processes that increase the bioavailability of calcium in milk probably also affect barium (because of the chemical similarity between the two elements[17]), which would lead to greater absorption of barium from milk compared to non-milk foods.

We estimate that the mineralization of the upper and lower *A. afri- canus* first molars (M^1 and M_1, respectively) from specimen StS 28 and a lower canine from specimen StS 51 started soon after and about three months after birth, respectively[18]. To preserve these samples, thin sections of the teeth were not created and developmental timing of the tooth samples were estimated using known values[18,19]. Both teeth show an increasing Ba/Ca ratio from the start of mineralization, which peaks at six

and nine months for StS 28 M^1 molar and StS 51 lower canine, respectively, on the basis of crown formation times[18,19]. This indicates a diet predominated by breast milk (Fig. 1) for a minimum of 6–9 months, followed by increased supplementation with non-milk foods (which peak at around 12 months). After the initial deposition at a high Ba/Ca ratio, the elemental ratio increases and decreases in a cyclical pattern that has a period of about 4–6 months for StS 51 (Figs. 1–3, Extended Data Fig. 4) and 6–9 months for StS 28 (Figs. 1, 2, Extended Data Fig. 3). The cyclical signal is clearly visible in all of the *A. africanus* teeth that we analysed, with multiple occurrences from cusp to root that follow a pattern that is associated with tooth growth rather than diagenesis, and which are consistent across teeth from the same individual. Uranium (a marker of diagenesis) shows a diffuse pattern that does not follow tooth growth patterns, which is markedly different from the pattern of the Ba/Ca ratio. Although the presence of uranium indicates some post-burial alteration, the presence of barium, strontium and lithium banding that follows the developmental architec- ture of dentinogenesis and amelogenesis, and the repetition of the pat- tern across teeth from the same individual, confirms that the observed cyclical patterns are biogenic (Extended Data Figs. 3, 4, Supplementary Discussion). The highly cyclical Ba/Ca pattern observed in permanent teeth from StS 28 and StS 51 indicates a repeated behaviour over time until at least about 4–5 years of age (Figs. 1–3, Extended Data Figs. 3, 4). This pattern is reinforced by Sr/Ca and Li/Ca signals, which also occur cyclically along the growth axis of the tooth. A similar recurring pattern in Li/Ca, Ba/Ca and Sr/Ca ratios has previously been observed in modern wild orangutans (both *Pongo abelii* and *Pongo pygmaeus*)[5] up to nine years of age. This pattern has been interpreted as seasonal dietary adaptation, in which Ba/Ca ratios in teeth increased when infants relied more heavily on their mother's milk during periods of low food availability. To investigate further, we analysed teeth from several modern mammals from a similar ecological landscape (Extended Data Fig. 5) to that of *A. africanus*. All of these teeth also showed cyclical Ba/Ca signals. Although no reliable crown formation times could be sourced for these mammals (Supplementary Table 1), they are reported to wean at a young age (between 2 and 9 months, or up to 12 months for baboons)[15]. This suggests that the cyclical pattern shown in the teeth of mammals living in grass- land-dominated ecosystems reflects seasonal dietary adaptations; later periods of higher Ba/Ca ratios may indicate increased consumption of another, non-milk source of highly bioavailable barium. The recurring pattern was least noticeable in carnivores, which suggests that these animals show less variation in their diet. A cycle of about eight months was estimated in the baboon, which is notably similar to that observed in *A. africanus* (Extended Data Fig. 6a). Additionally, the Ba/Ca value measured in the modern baboon first molar is higher than for the third molar, which may reflect a mixture of the seasonal dietary oscillation and milk intake signals in the first molar compared to only the seasonal dietary oscillation signal in the third molar (Extended Data Fig. 6b). However, the possibility that differences in mineralization and the physiological cycle during amelogenesis had a role in generating the difference in values cannot be excluded. Although the Ba/Ca banding in *A. africanus* appears to have greater regularity than that in the mod- ern mammals (in particular for the StS 28 M^1 molar), the number of samples and lack of accurate tooth-age estimates limits further analysis of any variation in seasonal regularity between modern environments and those of the early Pleistocene epoch.

In general, Sr/Ca banding was clearer across the teeth in *A. africanus* and showed additional narrow lines that were not observable in the Ba/ Ca images (Extended Data Figs. 3, 4). However, the Sr/Ca and Ba/Ca patterns were largely synchronous, which indicates a common source of exposure (Extended Data Figs. 5, 6). This is in contrast to modern human samples, which often show asynchronous Ba/Ca and Sr/Ca pat- terns (Extended Data Fig. 7). Li/Ca banding in teeth from *A. africanus* the patterns of teeth from wild orangutans (Extended Data Fig. 10). Narrow bands of increased barium and strontium were observed in this captive orangutan; we attribute them to acute stress events[24]. Intense narrow barium and strontium bands were also observed in teeth from *A. africanus*, baboons and other savannah mammals; however, these bands overlap with broader dietary bands, which indicates a co-occurrence of stress and seasonal dietary changes. The overlap of possible cyclical nursing and a stressful environment due to changing food availability make it difficult to accurately interpret the underlying cause of the banding pattern (Extended Data Fig. 6a).

Similarly, the Li/Ca banding pattern—which is also found in modern orangutans and (to a lesser extent) baboons, but is rarely observed in modern *Homo* samples (Extended Data Fig. 7) or in the non-primate mammals that we analysed—suggests complex physiological adaptations to cyclical periods of abundance and star- vation. Although lithium is not directly incorporated within the fatty was less frequent than the other elemental patterns that we observed, but occurred predominantly just before the highest-amplitude Ba/Ca intake episodes (Fig. 2, Extended Data Fig. 8). Furthermore, this rela- tionship between the two cycles was not observed in the non-primate mammals that we analysed (Extended Data Fig. 5), but was detected in both modern baboons and modern orangutans[5]. The presence of highly cyclical Ba/Ca and Li/Ca banding in *A. africanus* probably reflects sea- sonal dietary shifts, and perhaps also physiological responses similar to those of modern wild orangutans[5]. It appears that *A. africanus* under- went seasonal food stress, and had to adapt to changing resources and food access[20]. The analysis of the strontium isotope ratio ($^{87}Sr/^{86}Sr$) of *A. africanus* from Sterkfontein shows that some individuals lived principally on the dolomite karst, which was dominated by more-open bushland and grassland (instead of the closed woodland characteristic of surrounding lithologies)[3,10,11]. Our strontium isotope data (Extended Data Fig. 9) are consistent with the scenario in which both of the indi- viduals that we analysed spent the majority of their time in the Malmani Dolomite Subgroup during amelogenesis. This specific geological set- ting is severely depleted in many nutrients, which limits plant growth[8]. Some primate species opportunistically adapted their physiology to cope with seasonal food availability due to specific environmen- tal pressures[21]. Immature baboons in high-altitude environments—a challenging setting for offspring—have been reported to extend their nursing cycles, decrease their foraging time, wean later and engage in lower-energy activity than lowland baboons[21]. Varying milk intake can compensate for periods of extreme, and unpredictable, oscillations in food availability. This adaptation enables the survival of immature individuals, who are particularly vulnerable to fluctuations in food accessibility because of their lower fat reserves and weaker muscle tis- sues. During periods of abundance the infant can rely more heavily on solid food, which allows the mother to replenish her energetic and calcium reserves to support an increase in lactation during periods of food scarcity. Previous reports have suggested that wild orangutan (*P. abelii* and *P. pygmaeus*) females have adapted to seasonal variation by increasing the weaning period until an offspring age of 8–9 years old[5]. This ecological exigency has forced orangutan females to lower their metabolic requirements[20], increase their ability to rapidly build energetic reserves[22] and to catabolize fat reserves and muscle tissue faster during periods of nutrient insufficiency[23]. Elemental mapping of a tooth from a captive orangutan that received a constant supply of food showed a pattern that lack imprints of cyclical dietary intake, unlike tissues, this element has been shown to vary in concentration with body mass[25]. However, the exact relationship between weight gain and lithium storage remains unclear; in modern humans, there is a possible link between lithium storage, weight gain and psychological factors (Supplementary Discussion). Another

explanation could be the role of lithium in preventing protein deficiency during periods of low caloric intake[26]. Primates are known to switch to fall-back foods with a higher protein content during seasonal resource scarcity, to maintain their strength[20,22]. Moreover, lithium concentration can vary greatly between individual plants, or between parts of the same plant, and has been reported to transfer to breast milk (Supplementary Discussion). Although evidence for an adaptive shift to fall-back resources in *A. afri- canus* has been questioned[8,9,27], the periodic lithium signal (which is compatible with seasonal changes[28]) might suggest the existence of such an adaptive trait. During periods of severe food shortage, immature australopithecines might have developed physiological adaptations to compensate for low caloric intake from fall-back resources, which perhaps included a long weaning sequence. Undoubtedly, the high Ba/Ca and Li/Ca ratio bands in *A. africanus* dental tissues attest to a strong seasonal oscillation in food access, which would have had a substantial effect on australopithecine development. This interpretation is reinforced by the high frequency of developmental defects in the enamel of this species, which was the result of nutritional deficiencies[29]. Our elemental analysis suggests *A. africanus* had a short period (not exceeding a year) during which breastfeeding was predominant, which is a very different sequence to that of extant great apes and instead represents a timing that is comparable with modern *Homo* species[4,30]. Because nursing and seasonal dietary banding cannot be precisely disentangled, it remains possible that the species retained a weaning sequence well into advanced offspring age to overcome seasonal food shortages, similar to modern great apes[5,30]. Our results have identified important dietary cycles and physiological adaptations in response to food access, which would have had considerable repercussions for the social structures and ecological behaviours adopted by groups of *A. africanus*. These adaptations in response to seasonal variability and resource scarcity would have extracted a toll on the resilience to other environmental pressures, and thus possibly had a role in the disappear- ance of the genus from the fossil record at about 2 Ma[6].

1. Balter, V., Braga, J., Télouk, P. & Thackeray, J. F. Evidence for dietary change but not landscape use in South African early hominins. *Nature* **489**, 558–560 (2012).
2. Ungar, P. S. & Sponheimer, M. The diets of early hominins. *Science* **334**, 190–193 (2011).
3. Copeland, S. R. et al. Strontium isotope evidence for landscape use by early hominins. *Nature* **474**, 76–78 (2011).
4. Austin, C. et al. Barium distributions in teeth reveal early-life dietary transitions in primates. *Nature* **498**, 216–219 (2013).
5. Smith, T. M., Austin, C., Hinde, K., Vogel, E. R. & Arora, M. Cyclical nursing patterns in wild orangutans. *Sci. Adv*. **3**, e1601517 (2017).
6. Herries, A. I. R. et al. in *The Paleobiology of* Australopithecus *(Vertebrate Paleobiology and Paleoanthropology Series)* (eds Reed, K. E. et al.) 21–40 (Springer, Dordrecht, 2013).
7. Peterson, A., Abella, E. F., Grine, F. E., Teaford, M. F. & Ungar, P. S. Microwear textures of *Australopithecus africanus* and *Paranthropus robustus* molars in relation to paleoenvironment and diet. *J. Hum. Evol*. **119**, 42–63 (2018).
8. Sponheimer, M. & Lee-Thorp, J. A. Isotopic evidence for the diet of an early hominid, *Australopithecus africanus*. *Science* **283**, 368–370 (1999).
9. Strait, D. S. et al. The feeding biomechanics and dietary ecology of *Australopithecus africanus*. *Proc. Natl Acad. Sci. USA* **106**, 2124–2129 (2009).
10. Dupont, L. M., Donner, B., Vidal, L., Pérez, E. M. & Wefer, G. Linking desert evolution and coastal upwelling: Pliocene climate change in Namibia. *Geology* **33**, 461–464 (2005).
11. Pickering, R. & Herries, A. I. R. in *Hominin Postcranial Remains from Sterkfontein, South Africa* (eds Ward, C. V. & Zipfel, B.) (Oxford Univ. Press, Oxford, in the press).
12. Clarke, R. in *The Paleobiology of* Australopithecus *(Vertebrate Paleobiology and Paleoanthropology Series)* (eds Reed, K. et al.) 105–123 (Springer, Dordrecht, 2013).
13. Ecker, M., Brink, J., Kolska-Horwitz, L., Scott, L. & Lee-Thorp, J. A. A. 12,000 years record of changes in herbivore niche separation and palaeoclimate (Wonderwerk Cave, South Africa). *Quat. Sci. Rev*. **180**, 132–144 (2018).
14. Caley, T. et al. A two-million-year-long hydroclimatic context for hominin evolution in southeastern Africa. *Nature* **560**, 76–79 (2018).
15. Shorrocks, B. *The Biology of African Savannas* (Oxford Univ. Press, New York, 2007).
16. Krachler, M., Rossipal, E. & Micetic-Turk, D. Concentrations of trace elements in sera of newborns, young infants, and adults. *Biol. Trace Elem. Res*. **68**, 121–135 (1999).
17. Bouhallab, S. & Bouglé, D. Biopeptides of milk: caseinophosphopeptides and mineral bioavailability. *Reprod. Nutr. Dev*. **44**, 493–498 (2004).
18. Smith, T. M. et al. Dental ontogeny in Pliocene and Early Pleistocene hominins. *PLoS ONE* **10**, e0118118 (2015).
19. Lacruz, R. S., Dean, M. C., Ramirez-Rozzi, F. & Bromage, T. G. Megadontia, striae periodicity and patterns of enamel secretion in Plio-Pleistocene fossil hominins. *J. Anat*. **213**, 148–158 (2008).
20. Pontzer, H., Raichlen, D. A., Shumaker, R. W., Ocobock, C. & Wich, S. A. Metabolic adaptation for low energy throughput in orangutans. *Proc. Natl Acad. Sci. USA* **107**, 14048–14052 (2010).
21. van Noordwijk, M. A., Willems, E. P., Utami Atmoko, S. S., Kuzawa, C. W. & van Schaik, C. P. Multi-year lactation and its consequences in Bornean orangutans (*Pongo pygmaeus*). *Behav. Ecol. Sociobiol*. **67**, 805–814 (2013).
22. Vogel, E. R. et al. Bornean orangutans on the brink of protein bankruptcy. *Biol. Lett*. **8**, 333–336 (2012).
23. Harrison, M. E., Morrogh-Bernard, H. C. & Chivers, D. J. Orangutan energetics and the influence of fruit availability in the nonmasting peat-swamp forest of Sabangau, Indonesian Borneo. *Int. J. Primatol*. **31**, 585–607 (2010).
24. Austin, C. et al. Uncovering system-specific stress signatures in primate teeth with multimodal imaging. *Sci. Rep*. **6**, 18802 (2016).
25. Gitlin, M. Lithium side effects and toxicity: prevalence and management strategies. *Int. J. Bipolar Disord*. **4**, 27 (2016).
26. Tandon, A., Bhalla, P., Nagpaul, J. P. & Dhawan, D. K. Effect of lithium on rat cerebrum under different dietary protein regimens. *Drug Chem. Toxicol*. **29**, 333–344 (2006).
27. Wood, B. & Schroer, K. Reconstructing the diet of an extinct hominin taxon: the role of extant primate models. *Int. J. Primatol*. **33**, 716–742 (2012).
28. Potts, R. Paleoenvironmental basis of cognitive evolution in great apes. *Am. J. Primatol*. **62**, 209–228 (2004).
29. Guatelli-Steinberg, D. Macroscopic and microscopic analyses of linear enamel hypoplasia in Plio-Pleistocene South African hominins with respect to aspects of enamel development and morphology. *Am. J. Phys. Anthropol*. **120**, 309–322 (2003).
30. Kennedy, G. E. From the ape's dilemma to the weanling's dilemma: early weaning and its evolutionary context. *J. Hum. Evol*. **48**, 123–145 (2005).

Methods

Geochemical mapping. The fossil teeth StS 28 ($n = 3$) and StS 51 ($n = 2$) (and all other specimens presented in this paper) were sectioned with a high-precision diamond saw at the apex of the cusp, then surface-polished to 10-⌈m smoothness (Extended Data Figs. 2, 3). Each tooth was then introduced into the laser-ablation inductively coupled-plasma mass spectrometry (LA-ICP-MS) chamber for analysis (Extended Data Fig. 4). LA-ICP-MS was used for trace-element mapping analyses of the sample, according to a published protocol previously used for Neanderthal breastfeeding analyses[4]. SOLARIS at Southern Cross University (ESI NWR213 coupled to an Agilent 7700 ICP-MS), and a separate system at Icahn School of Medicine at Mount Sinai in New York (ESI NWR193 ArF excimer laser coupled to an Agilent 8800 ICP-MS), were used to map the samples, with the laser beam

rastered along the sample surface in a straight line. The laser spot size was 40 ⌈m or 35 ⌈m, the laser scan speed was 80 ⌈m s^{-1} or 70 ⌈m s^{-1}, and the laser intensity was 80% or 60%, respectively, and an ICP-MS total integration time of 0.50 s pro- duced data points that corresponded to a pixel size of approximately 40 · 40 ⌈m or 35 · 35 ⌈m, respectively. NIST610, NIST612 and NIST614 (certified standard reference materials) were used to assess signal drift.

Isotopic profiling. $^{87}Sr/^{86}Sr$ was measured by a laser-ablation multi-collector inductively coupled plasma mass spectrometer (LA-MC-ICP-MS) at the University of Wollongong

(WIGL laboratory) (Thermo Neptune Plus connected to an ESI NWR193 ArF excimer laser ablation system). Both enamel and dentine of StS 28 and StS 51 were analysed with nine and six 150-⌈m ablation spots (respectively), a dwell time of 50 s, 20-Hz frequency and 40% laser intensity. Sample aerosol was carried to the ICP-MS using a mixture of He and N_2. The following isotopes were collected in static mode: ^{82}Kr, ^{83}Kr, ^{84}Sr, ^{85}Rb, ^{86}Sr, $^{172}Yb^{2+}$, ^{87}Sr, ^{88}Sr and $^{177}Hf^{2+}$. Each isotope was collected using cycles of 1 s each. Data reduction (including a background subtraction, mass bias, Rb/Sr and Ca argide/dimer corrections) were performed using Iolite[31] with the Ca–Ar interference correction Sr isotope scheme[32]. A seal tooth and a clam shell with modern seawater $^{87}Sr/^{86}Sr$ value (0.7092)[33] were analysed four times at the start and end of each session and used as a matrix-matched primary standard to further correct the $^{87}Sr/^{86}Sr$ ratios.

Image processing. For elemental maps obtained by LA-ICP-MS, ablation lines were extracted in the form of .csv files generated by the MassHunter Workstation software (Agilent). Each file was then imported into the interactive R Shiny applica- tion 'shinyImaging' (the application can be accessed by contacting the correspond- ing author or at http://labs.icahn.mssm.edu/lautenberglab/), which transforms each isotope into a separate file that contains the counts per second values of one element and is organised as a matrix (number of ablation lines multiplied by the number of ablation spots per ablation line). For each element, gas blank counts per second (median value in pixels per ablation spot) collected during the first 10 s of each analysis (gas blank) were used as background and subtracted from the rasterstack. Background signal around the teeth (arising from the encasing resin) was converted to white coloration (no intensity) to increase clarity of the figures, by isolating the dental tissue from its surroundings. Colour scales were applied using the linear blue–red Lookup Table. For Fig. 3c, the enamel and dentine of the StS 51 canine were set at a slightly different scale to enable clearer identification of the different bands, and the sliding coloured scale was adjusted accordingly.

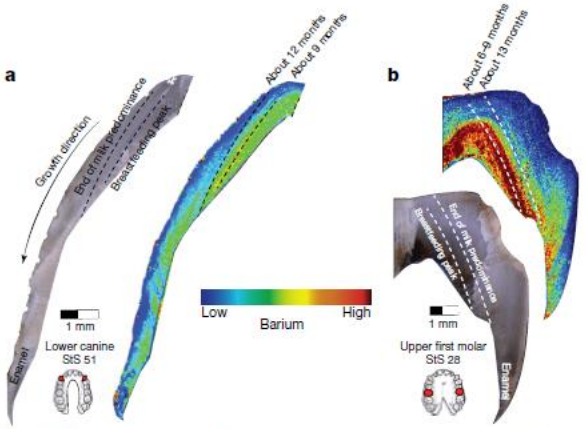

Fig. 1 | Breastfeeding period of *A. africanus*. **a**, Section of enamel of the lower canine of StS 51, and associated $^{138}Ba/^{43}Ca$ elemental mapping. **b**, Section of the enamel of the upper first molar of StS 28, and associated $^{138}Ba/^{43}Ca$ elemental mapping. The dotted lines indicate the beginning of enamel calcification, the time at which the breastfeeding peaked and the date at which the infant *A. africanus* breast milk intake decreased with respect to solid food intake. A period of approximately 12 and 13 months for StS 51 and StS 28, respectively, for predominant breastfeeding was estimated using the distance between the identified lines and the average rate of calcification of the species (5.5 μm d^{-1})[16–18].

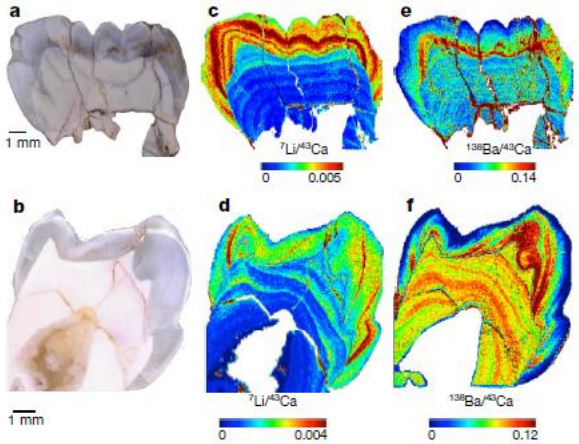

Fig. 2 | Elemental mapping of *A. africanus* StS 28 and StS 51 fossil teeth. **a**, **b**, Micrograph (10× magnification) of StS 28C permanent first molar (**a**) and StS 51A permanent first premolar (P3) (**b**). **c**–**f**, Associated elemental mapping of $^{7}Li/^{43}Ca$ StS 28 (**c**) and StS 51 (**d**) and $^{138}Ba/^{43}Ca$ StS 28 (**e**) and StS 51 (**f**). Assuming similar timings for tooth development in *A. africanus* and *Homo*, the crown formation of the permanent first molar would correspond to an early-life record from birth to about 7 years of age, and the crown formation of the permanent first premolar would correspond to an early-life record from 1.5 years to about 5 years of age.

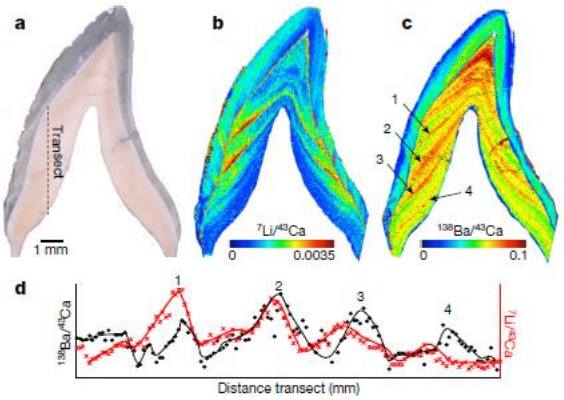

Fig. 3 | Elemental mapping of StS 51 *A. africanus* canine. **a**, Micrograph (10× magnification) of StS 51B permanent lower canine. **b**, **c**, Associated elemental mapping of $^{7}Li/^{43}Ca$ (**b**) and $^{138}Ba/^{43}Ca$ (**c**). Permanent canine teeth develop only a few months after birth, with completion of the crown between three and four years of age[18]. **d**, Comparison of the temporal periodicity of Ba/Ca (black line and diamonds) and Li/Ca (red line and crosses) accentuated lines (labelled 1, 2, 3 and 4), along the transect illustrated in **a**. Li/Ca recurrence shows a slight temporal offset compared to Ba/Ca periodicity.

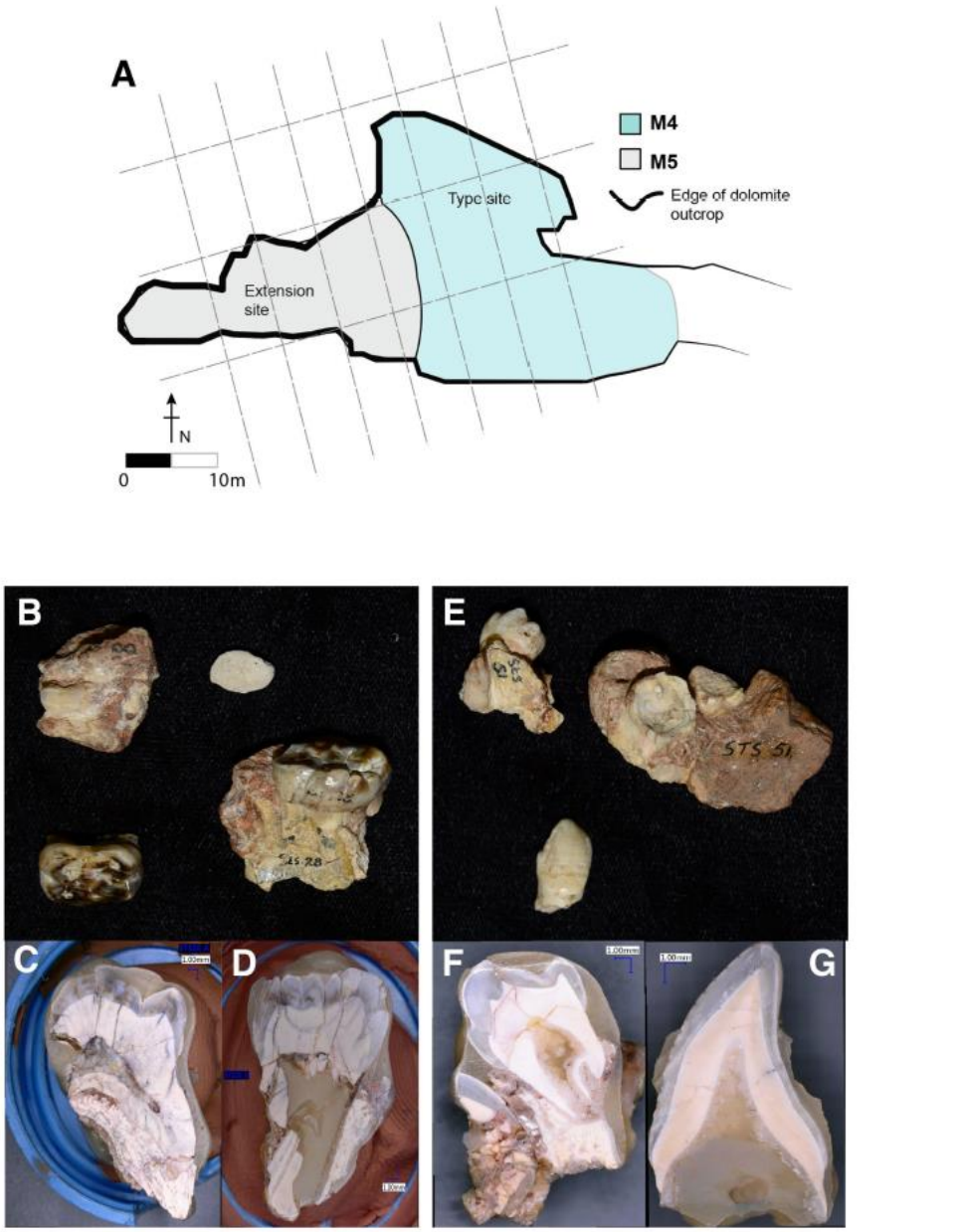

Extended Data Fig. 1 | The Sterkfontein surface excavation and fossil teeth specimen. a, Plan view of the Sterkfontein surface excavation (adapted from ref. [34]) showing the association between the type site excavation and Member 4 deposits. **b**, Photograph of fossil teeth of specimen StS 28. **c**, Upper first molar (M1) StS 28B. **d**, Permanent lower first molar (M1) StS 28C, after being sectioned in two with a diamond low-speed high-precision rotary saw. **e**, Photograph of fossil teeth of specimen StS 51. **f**, Permanent premolar (P3) StS 51A. **g**, Permanent canine (LC) StS 51B, after being sectioned in two with a diamond low-speed high-precision rotary saw. The two teeth that are still embedded in the breccia were not sectioned.

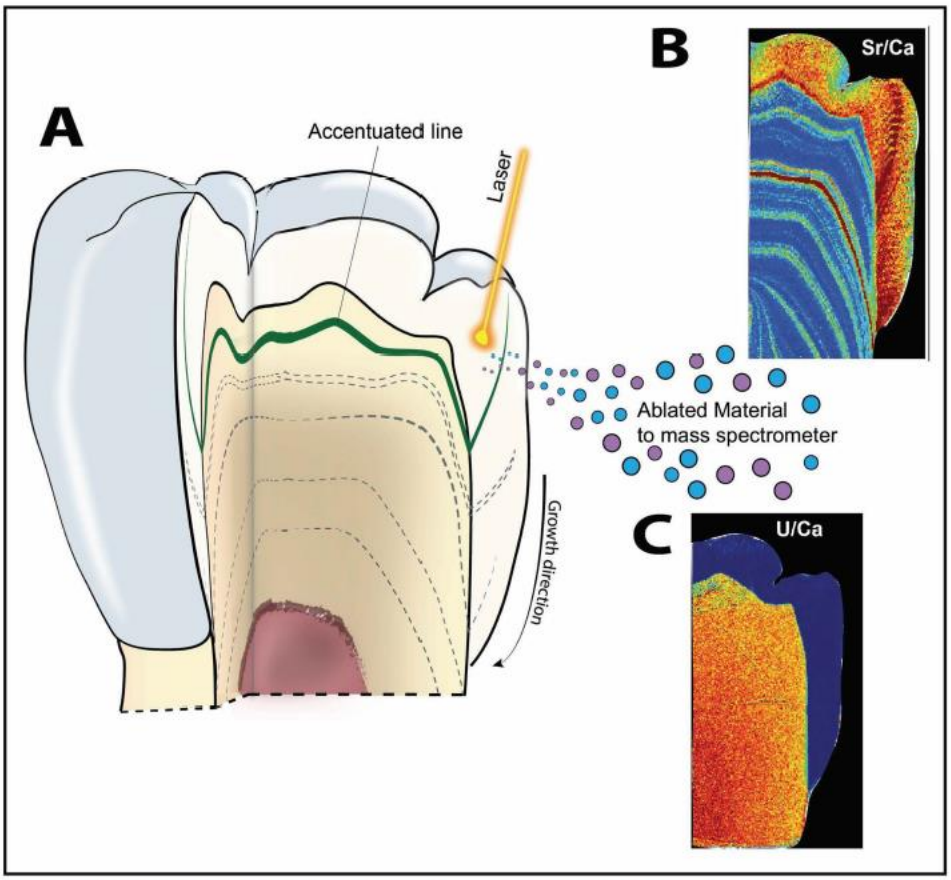

Extended Data Fig. 2 | Elemental mapping protocol. a, Sketch of second molar tooth dentine and enamel section (with indication of biogenic accentuated lines in green) of a fossil *Pongo* sp. **b**, **c**, Elemental mapping of both dental tissues using LA-ICP-MS shows strontium distribution following the incremental growth pattern of the tooth (**b**), typical of biogenic signals, contrary to post-mortem diagenetic processes (**c**) (uranium diffusion during burial).

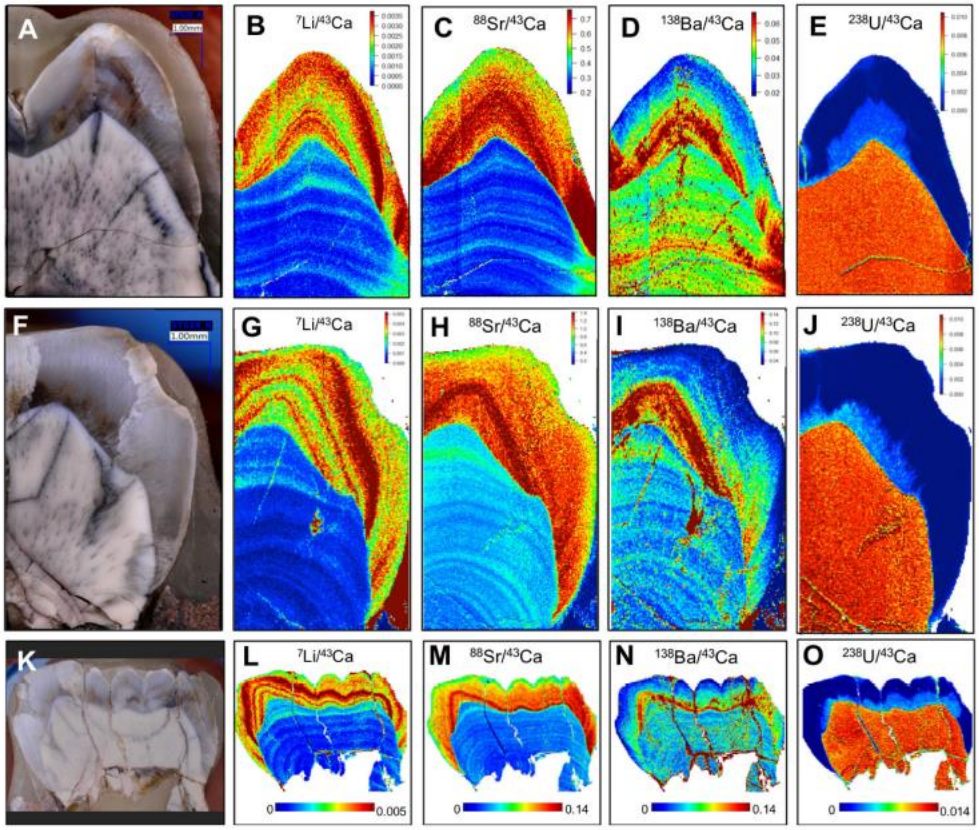

Extended Data Fig. 3 | Elemental mapping of *A. africanus* StS 28. **a**–**o**, Elemental mapping of upper first molar cusp (StS 28B) (**a**–**e**); and lower first molar (StS 28C) (**f**–**o**), showing records of cyclical banding between zero and seven years at crown completion. The broad repeated banding pattern is attributed to seasonal dietary shifts, and potentially to cyclical nursing during long weaning periods. The identical elemental banding pattern that is found in both the StS 28B and StS 28C first permanent molars confirm the biogenic nature of the signal observed (compare **b**, **c** and **d** with **g**, **h** and **i**, respectively). The typical patchy and spreading diffusion pathways of uranium in the dentine and the enamel can be observed (**e**, **j** and **o**) with characteristic accumulation or depletion in cracks and at the enamel–dentine junction, which is very different to the biogenic lithium, strontium and barium banding.

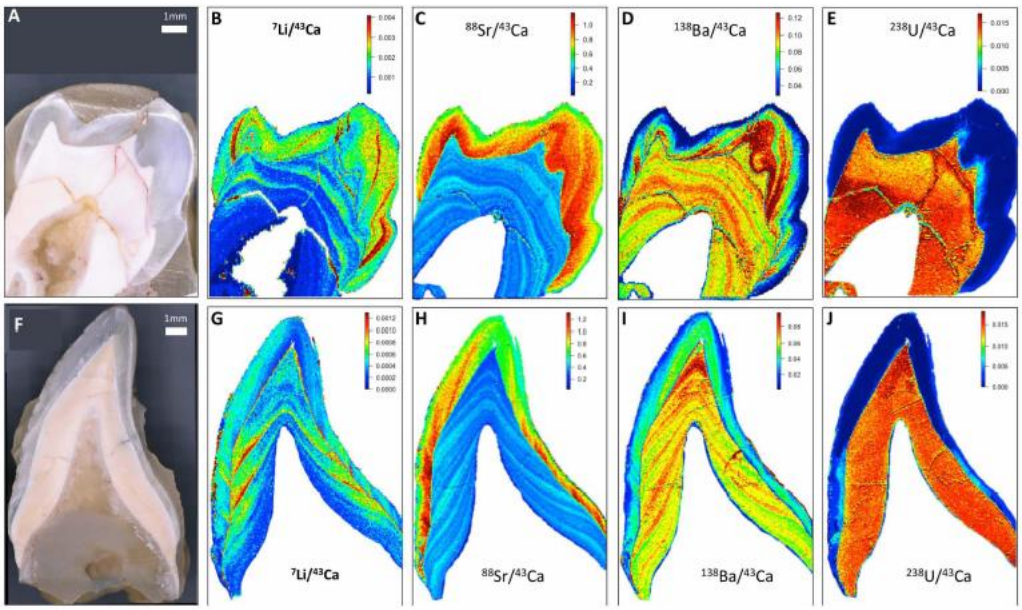

Extended Data Fig. 4 | Elemental mapping of *A. africanus* StS 51. **a**–**e**, Photograph (**a**) and elemental mapping of permanent premolar StS 51A Li/Ca banding (**b**), Sr/Ca banding (**c**), Ba/Ca banding (**d**) and U/Ca diffusion (**e**). **f**–**j**, Photograph (**f**) and elemental mapping of permanent canine (StS 51B) Li/Ca banding (**g**), Sr/Ca banding (**h**), Ba/Ca banding (**i**) and U/Ca diffusion (**j**). The strontium signal shows additional discrete lines (that are most likely to be associated with episodes of stress) compared to Li/Ca and Ba/Ca. Uranium distribution shows a typical and rather uniform diffusion pattern with enrichment close to the enamel–dentine junction and in fractures and cracks.

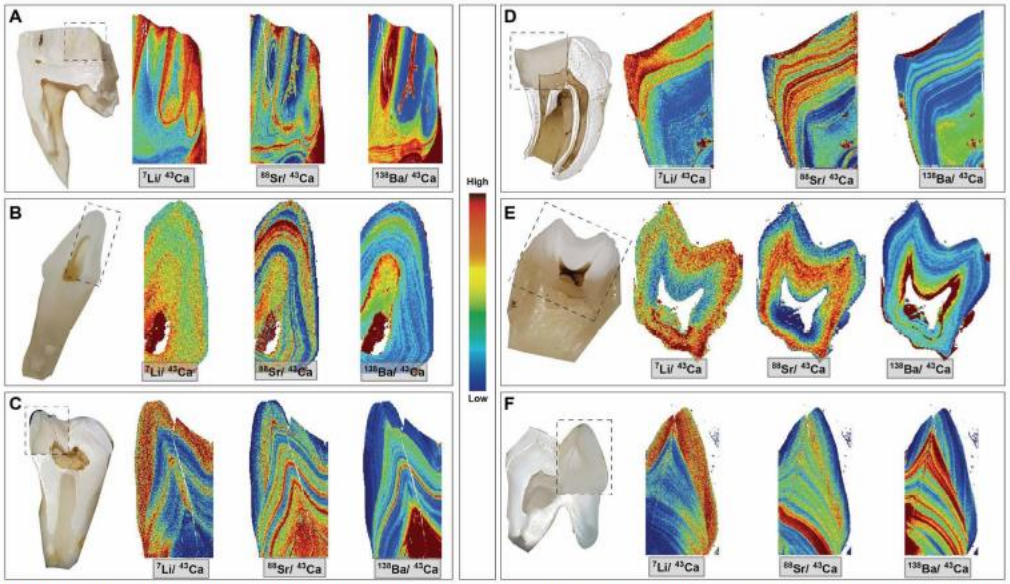

Extended Data Fig. 5 | LA-ICP-MS trace-element mapping of primate and non-primate mammals. a–f, All teeth specimens are from the grassland-dominated ecosystem of South Africa (frequently referred as savannah) and were recovered from wild, modern animals. **a**, M2 molar of springbok (*Antidorcas marsupialis*; herbivore). **b**, P4 premolar of caracal (*Caracal caracal*; carnivore). **c**, Third molar (M3) of chacma baboon (*Papio ursinus*; omnivore). **d**, First premolar (P3) of red river hog (*Potamochoerus porcus*; omnivore). **e**, Second molar (M2) of bat-eared fox (*Otocyon megalotis*; insectivore/carnivore). **f**, *P. ursinus* first molar (M1). All mammals exhibit Ba/Ca and Sr/Ca banding (except for **e**, in which no strontium lines can be observed). Li/Ca banding is absent from animal teeth except from the two *P. ursinus* teeth (**c**, **f**) and—perhaps—the *P. porcus* tooth (**d**). The Ba/Ca banding pattern in *Papio* is very similar to that observed in *A. africanus*: apart from the lack of clear periodicity, the baboon teeth are comparable to those of *A. africanus*. Baboons have a unique nursing cycle and an opportunistic seasonal feeding habit.

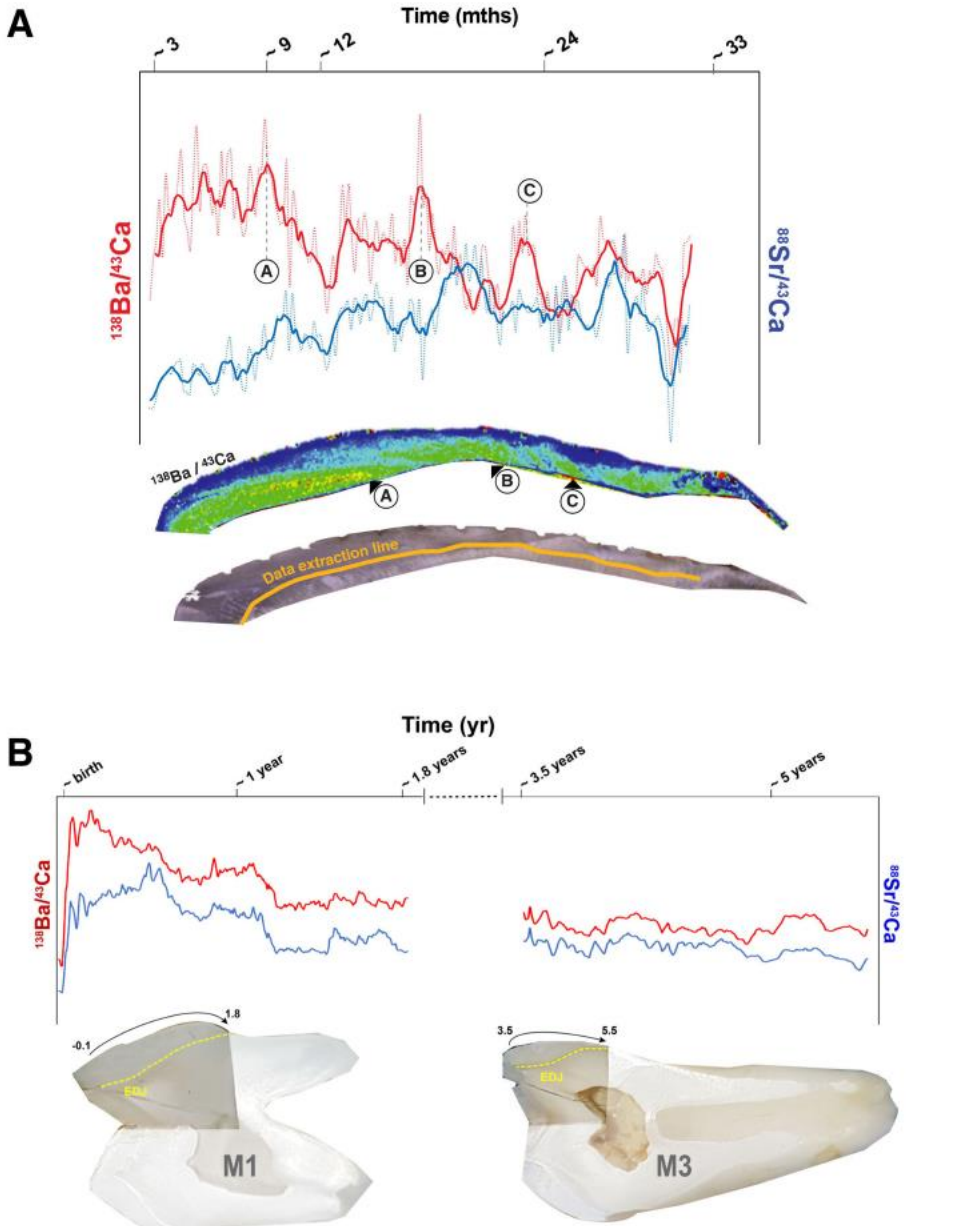

Extended Data Fig. 6 | $^{138}Ba/^{43}Ca$ and $^{88}Sr/^{43}Ca$ distribution in the enamel parallel to the enamel–dentine junction. a, StS 51 canine. The comparison of Ba/Ca and Sr/Ca ratios shows an inverse correlation towards the end of exclusive breastfeeding (marked by a circled A). This pattern is repeated at the points marked by circled B and C; these are approximately six months apart, which may indicate cyclical milk intake. The concurrent increase in Sr/Ca with decreasing Ba/Ca at the position marked by the circled A indicates an increase in the predominance of solid food in the diet, and a food source with more bioavailable strontium than is present in milk. The timing for the tooth development was approximated using estimated values for the species *A. africanus*[17,18], and assuming linear growth rate of the enamel. **b**, Modern baboon (*P. ursinus*) molars. The Ba/Ca and Sr/Ca ratios along the enamel–dentine junction of a first (left) (see also Extended Data Fig. 5f) and a third molar (right) (see also Extended Data Fig. 5c) of a modern baboon was compared, giving several years of record. Although both teeth had clear banding, the M1 molars display more intense fluctuations, compared to the pattern observed in the third molars. This is potentially attributable to an additional nursing signal in M1, with exclusive breastfeeding for the first 4–6 months, until being completely weaned at just after a year.

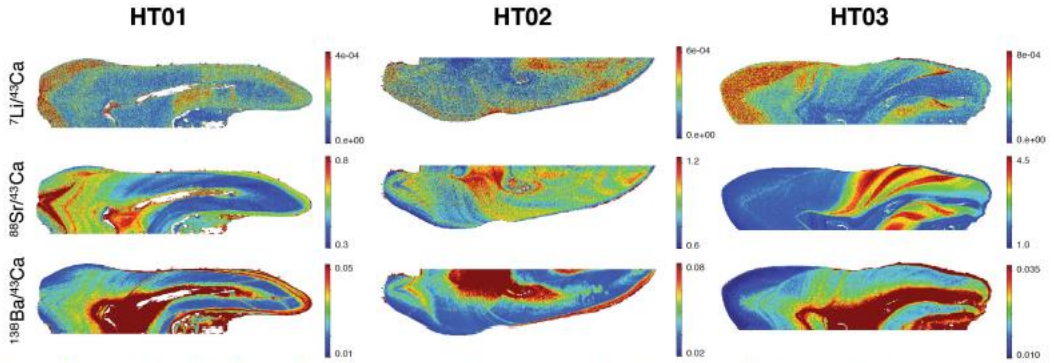

Extended Data Fig. 7 | LA-ICP-MS trace-element mapping of modern humans. The $^{7}Li/^{43}Ca$, $^{88}Sr/^{43}Ca$ and $^{138}Ba/^{43}Ca$ ratios for each of three modern human specimens (*Homo sapiens*), labelled HT01 (upper first molar), HT02 (lower first molar) and HT03 (upper first molar) (left to right, respectively). The distribution pattern of all three elements is notably different to the signal observed in *A. africanus*, with enrichment towards the pulp cavity for both $^{88}Sr/^{43}Ca$ and $^{138}Ba/^{43}Ca$ that is probably associated with blood flow. An important difference is the absence of a repeated pattern that is observable for all three elemental ratios. Although some features could be interpreted as banding (such as the $^{88}Sr/^{43}Ca$ root signal of HT03), these isolated patterns are not mirrored in the distributions of the other elements.

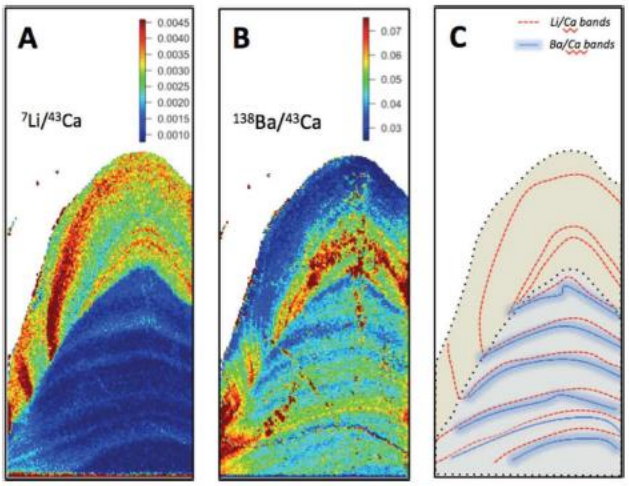

Extended Data Fig. 8 | Comparison of temporal occurrence of lithium and barium banding in the StS 28C upper first molar. a–c, The Li/Ca banding (**a**) when placed over the Ba/Ca bands (**b**) shows a slight offset of the lithium banding (**b**). The lighter element (red dotted line marks the start of the lithium deposition) appears to occur immediately before, and during, the deposition of Ba/Ca (blue shaded lines). We hypothesi that the location of lithium in the hydrosphere of the bone means that this element is more rapidly reabsorbed and transported into the bloodstream than is barium.

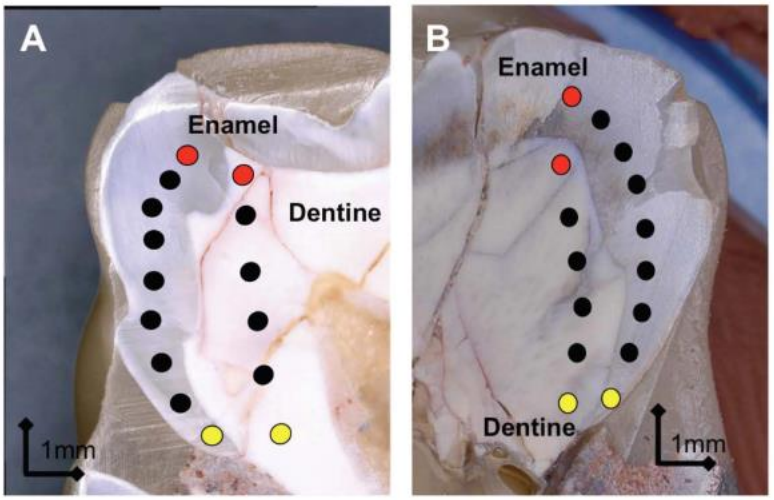

	STS 51				STS 28			
	Enamel		*Dentine*		*Enamel*		*Dentine*	
1	0.72693	0.00007	0.72901	0.00012	0.72832	0.00004	0.72868	0.00031
2	0.72709	0.00005	0.72740	0.00011	0.72819	0.00009	0.73121	0.00035
3	0.72594	0.00006	0.72753	0.00011	0.72832	0.00009	0.73082	0.00027
4	0.72655	0.00006	0.72787	0.00012	0.72844	0.00008	0.73197	0.00037
5	0.72575	0.00008	0.72813	0.00012	0.72834	0.00006	0.73248	0.00021
6	0.72699	0.00007	0.73190	0.00018	0.72922	0.00007	0.73428	0.00029
7	0.72577	0.00004	-	-	0.72991	0.00005	-	-
8	0.72636	0.00004	-	-	0.72972	0.00006	-	-
9	0.72689	0.00005	-	-	0.73130	0.00012	-	-

Extended Data Fig. 9 | Distribution of strontium isotopic ratio. **a**, **b**, Location of the laser-ablation spot (150 μm) along the enamel and dentine for StS 51A (**a**) and StS 28C (**b**). Circles with red filling correspond to the first point (1) and yellow filling to the final point (point 9 for enamel, and point 6 for dentine). The table below shows the $^{87}Sr/^{86}Sr$ isotopic ratio and associated errors for each laser-ablation spot measured above. All values measured in both teeth (including point 6 in the dentine of StS 28, with associated error) correspond to values of the Malmani dolomite that surrounds Sterkfontein (the $^{87}Sr/^{86}Sr$ ratio of the Malmani dolomite ranges between 0.723 and 0.734)[3], which shows that both specimens had limited mobility.

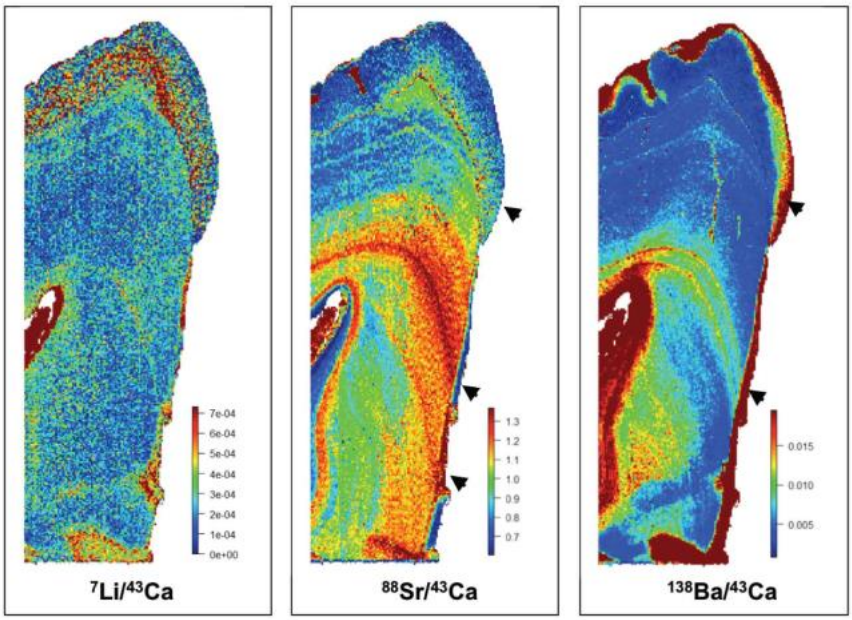

Extended Data Fig. 10 | Permanent second molar of a modern *Pongo* specimen from the Perth Zoo. The orangutan Hsing Hsing was born in captivity in 1975 in the Singapore Zoo, and was raised by its parents (although additional human feeding cannot definitively be excluded). The orangutan joined the Perth Zoo as an immature individual in 1983. There appears to be no Ba/Ca banding pattern that would indicate cyclical milk consumption during crown completion. The diet of this orangutan would have been substantially different to that of orangutans living in the wild, with limited seasonal influence and no periods of food scarcity. It is expected that the orangutan and its parents would have had abundant and guaranteed access to food, which would probably have led it to being prematurely weaned (as compared to wild *Pongo*). On this basis, it is unlikely that this orangutan would have had recurrent breastfeeding cycles, and therefore the absence of barium banding in this specimen is expected. The discrete banding lines observed in the Sr/Ca and the two Ba/Ca ratios are probably stress-related accentuated lines. No clear banding was observed in the enamel of this specimen.